Journal of the Neurological Sciences 347 (2014) 107–118

Contents lists available at ScienceDirect

Journal of the Neurological Sciences

journal homepage: www.elsevier.com/locate/jns

Lateralization of temporal lobe epilepsy by multimodal multinomial hippocampal response-driven models

Mohammad-Reza Nazem-Zadeh [a,b,*], Kost V. Elisevich [c], Jason M. Schwalb [d], Hassan Bagher-Ebadian [b,e], Fariborz Mahmoudi [a,b,f], Hamid Soltanian-Zadeh [a,b,g]

[a] Department of Research Administration, Henry Ford Health System, Detroit, MI 48202, USA
[b] Department of Radiology, Henry Ford Health System, Detroit, MI, 48202, USA
[c] Department of Clinical Neurosciences, Spectrum Health Medical Group, Grand Rapids, MI 49503, USA
[d] Department of Neurosurgery, Henry Ford Health System, Detroit, MI 48202, USA
[e] Department of Neurology, Henry Ford Health System, Detroit, MI 48202, USA
[f] Computer and IT engineering Faculty, Islamic Azad University, Qazvin Branch, Iran
[g] Control and Intelligent Processing Center of Excellence (CIPCE), School of Electrical and Computer, University of Tehran, Tehran, Iran

ARTICLE INFO

Article history:
Received 23 July 2014
Received in revised form 16 September 2014
Accepted 18 September 2014
Available online 28 September 2014

Keywords:
Temporal lobe epilepsy (TLE)
Hippocampus
Magnetic resonance imaging (MRI)
Single photon emission computed tomography (SPECT)
Multimodal multinomial response-driven lateralization models
Bayesian model averaging (BMA)

ABSTRACT

Purpose: Multiple modalities are used in determining laterality in mesial temporal lobe epilepsy (mTLE). It is unclear how much different imaging modalities should be weighted in decision-making. The purpose of this study is to develop response-driven multimodal multinomial models for lateralization of epileptogenicity in mTLE patients based upon imaging features in order to maximize the accuracy of noninvasive studies.
Methods and materials: The volumes, means and standard deviations of FLAIR intensity and means of normalized ictal–interictal SPECT intensity of the left and right hippocampi were extracted from preoperative images of a retrospective cohort of 45 mTLE patients with Engel class I surgical outcomes, as well as images of a cohort of 20 control, nonepileptic subjects. Using multinomial logistic function regression, the parameters of various univariate and multivariate models were estimated. Based on the Bayesian model averaging (BMA) theorem, response models were developed as compositions of independent univariate models.
Results: A BMA model composed of posterior probabilities of univariate response models of hippocampal volumes, means and standard deviations of FLAIR intensity, and means of SPECT intensity with the estimated weighting coefficients of 0.28, 0.32, 0.09, and 0.31, respectively, as well as a multivariate response model incorporating all mentioned attributes, demonstrated complete reliability by achieving a probability of detection of one with no false alarms to establish proper laterality in all mTLE patients.
Conclusion: The proposed multinomial multivariate response-driven model provides a reliable lateralization of mesial temporal epileptogenicity including those patients who require phase II assessment.

1. Introduction

Mesial temporal lobe epilepsy (mTLE) is the most prevalent type of epilepsy considered for surgery [1]. Reliable lateralization by noninvasive means would expedite surgical intervention, reduce the surgical risk of invasive monitoring and lessen the expense of investigation. Conventional noninvasive presurgical evaluation has often consisted of scalp electroencephalography (EEG), magnetic resonance imaging (MRI) and both ictal single photon emission computer tomography (SPECT) interictal SPECT to identify seizure onset in mTLE prior to a resection. In the imaging realm, quantitative methods have been applied to both MRI and SPECT with promising results to establish laterality in mTLE. Automated and manual hippocampal segmentation approaches for volume assessment have yielded 74% and 78% lateralization accuracy [2,3] whereas, fluid-attenuated inversion recovery (FLAIR) MRI signal analysis yielded a 98% accuracy in a single study [4]. Compartmentalized hippocampal SPECT analysis correctly lateralized mTLE in 91% of cases [5].

Where confident lateralization is not possible by qualitative assessment of these imaging modalities and individual quantitative measures of each do not provide effective differentiation, patients must undergo implantation of intracranial electrodes to clarify the situation [6] and must, in turn, bear the risk of such intervention [7]. An approach that would further capitalize on the benefits of the quantitative imaging approach [8] could serve to achieve the goals of improving patient safety and lessening cost.

* Corresponding author at: Tel.: +1 313 874 4349.
E-mail addresses: mohamadn@rad.hfh.edu (M.-R. Nazem-Zadeh), kost.elisevich@spectrumhealth.org (K.V. Elisevich), jschwal1@hfhs.org (J.M. Schwalb), hbagher1@hfhs.org (H. Bagher-Ebadian), fariborzm@rad.hfh.edu (F. Mahmoudi), hamids@rad.hfh.edu, hszadeh@ut.ac.ir (H. Soltanian-Zadeh).

http://dx.doi.org/10.1016/j.jns.2014.09.029
0022-510X/

A multimodal lateralization framework would ostensibly increase sensitivity and confidence in the lateralization of mTLE, if agreement was confirmed among individual imaging modalities. These modalities differ in their reliabilities and may, to some degree, show discrepancies in predicting laterality. The approach uniformly taken in these circumstances involves an assignment of a score of zero or one as a measure of this reliability in lateralizing a mTLE [9,10]. A weighted integration scheme, in which a probability is assigned to individual modalities as a measure of their reliability, may provide a more accurate reflection of laterality, particularly in those cases that ultimately require invasive monitoring. Multimodal postprocessing is defined as a simultaneous rendering of various modalities which are spatially coregistered [11]. It can incorporate all anomalous information of multiple modalities simultaneously without having to assign a posterior probability to the lateralization result of any individual modality.

Any variability in quantitative imaging indices can be attributed to natural physiological occurrences or pathology underlying the epileptogenicity. In order to distinguish these features, imaging indices of a cohort of control, nonepileptic subjects must be ascertained to account for the variability seen in natural circumstances. A multinomial response model that takes into account such natural variability would overcome the limitations of a binomial response model that does not.

We hypothesize that a quantitative multimodal multinomial response model, using a preferred list of MRI and SPECT attributes, will optimize lateralization of mTLE and the selection of surgical candidates while reducing the need for extraoperative electrocorticography (ECoG).

2. Methods

2.1. Patients and treatment

The current research study at Henry Ford Health System is federally regulated and approved by the Henry Ford Health System Institutional Review Board (IRB). Between June 1993 and June 2009, 113 patients with mTLE underwent resection of the mesial temporal structure. Only those cases with Engel class I outcomes were selected from this initial cohort. Subsequently, those patients were excluded for whom any of their T1-weighted and FLAIR MRI or SPECT ictal imaging and interictal imaging had not been acquired. Others, whose acquired images were contaminated by imaging artifact that compromised the quality of imaging attributes in or near the hippocampi, such as magnetic field inhomogeneity were also removed from consideration. Forty-five patients remained (17 males aged 42.6 ± 8.5 (mean ± std); 28 females aged 35.1 ± 11.4). The majority of cases achieved an Engel class Ia outcome (41 Ia, 2 Ib, 2 Id). Resections were performed on the left side in 28 patients and on the right in 17. Fifteen patients required ECoG as part of their investigation. Twenty control, nonepileptic subjects were also included in this study.

2.2. MRI and SPECT data acquisition

Preoperative MRI was acquired on a 1.5 T or a 3.0 T MRI system (Signa, GE, Milwaukee, USA) including coronal T1-weighted (using inversion recovery spoiled gradient echo, IRSPGR protocol) and coronal T2-weighted (using fluid attenuated inversion recovery, FLAIR protocol) images. For the 1.5 T MRI, T1-weighted imaging parameters were TR/TI/TE = 7.6/1.7/500 ms, flip angle = 20°, voxel size = 0.781 × 0.781 × 2.0 mm^3 and FLAIR imaging parameters were TR/TI/TE = 10002/2200/119 ms, flip angle = 90°, voxel size = 0.781 × 0.781 × 3.0 mm^3. For the 3.0 T MRI, T1-weighted imaging parameters were TR/TI/TE = 10.4/4.5/300 ms, flip angle = 15°, voxel size = 0.39 × 0.39 × 2.00 mm^3 and FLAIR imaging parameters were TR/TI/TE = 9002/2250/124 ms, flip angle = 90°, voxel size = 0.39 × 0.39 × 3.00 mm^3.

Patients underwent preoperative SPECT imaging with a triple-head Picker gamma camera 3000XP imaging system with high-resolution fan-beam collimators (Picker International, Inc., Cleveland Heights, OH) within 2 − 3 h after the injection of 99mT ethylcysteinate diethylester at a dose of 550 MBq. The energy window was set at 140 keV ± 7.5%. For ictal studies, the radiotracer was injected within 56 s of seizure onset. Interictal SPECT studies were performed when the patient had no documented seizure activity for at least 24 h. Total acquisition time was about 30 min. The images were reconstructed by filtered backprojection and then filtered with a Wiener filter into a 128 × 128 image matrix with a voxel size of 2.2 × 2.2 × 6.1 mm^3.

Control subjects underwent the same 3.0 T MRI system and T1-weighted and FLAIR images were acquired with the same parameters mentioned above. They also underwent SPECT imaging, with six receivingTechnetium-99 m (99mTc) ethylcisteinate dimer (ECD), and 14 receiving [99mTc]-labeled hexamethyl-propylene amine oxime (HMPAO).

2.3. MRI and SPECT image co-registration and feature extraction

For each of the 65 cases (45 mTLE patients and 20 control subjects), both left and right hippocampi were first segmented from manually drawn ROIs on T1-weighted images. The manually segmented hippocampi were then co-registered to both FLAIR and ictal and interictal SPECT images using a rigid registration technique (FLIRT; [12]; Fig. 1).

The four hippocampal imaging attributes used for this study were volume [4], mean and standard deviation of FLAIR intensity [4], and mean of normalized ictal–interictal SPECT intensity (the difference between ictal and interictal intensities normalized to the whole brain interictal mean value) [5].

2.4. Development of single lateralization response models

The extracted imaging features were incorporated into the development of four univariate (Models 1 to 4) and three multivariate (Models 5 to 7) single response models for lateralization of epileptogenicity. Imaging attributes were considered as independent variables whereas laterality (i.e., left and right in the case of mTLE patients and neutral for control subjects) was considered the dependent variable in the development of response models using multinomial logistic function regression [13]:

- Model 1 univariate attributes: hippocampal volumes
- Model 2 univariate attributes: means of FLAIR intensity in left and right hippocampi
- Model 3 univariate attributes: standard deviations of FLAIR intensity in left and right hippocampi
- Model 4 univariate attribute: means of normalized “ictal interictal” SPECT intensity in left and right hippocampi
- Model 5 bivariate attributes: means and standard deviations of FLAIR intensity in left and right hippocampi
- Model 6 multivariate attributes: volumes, means and standard deviations of FLAIR intensity in left and right hippocampi
- Model 7 multivariate attributes: volumes, means and standard deviations of FLAIR intensity and means of normalized “ictal − interictal” SPECT intensity in left and right hippocampi

In order to assess how the multinomial logistic function generalized to an independent data set and how accurately this response model performed in practice, a cross-validation was performed using leave-one-out for sixty-five repetitions considering a single case as validation

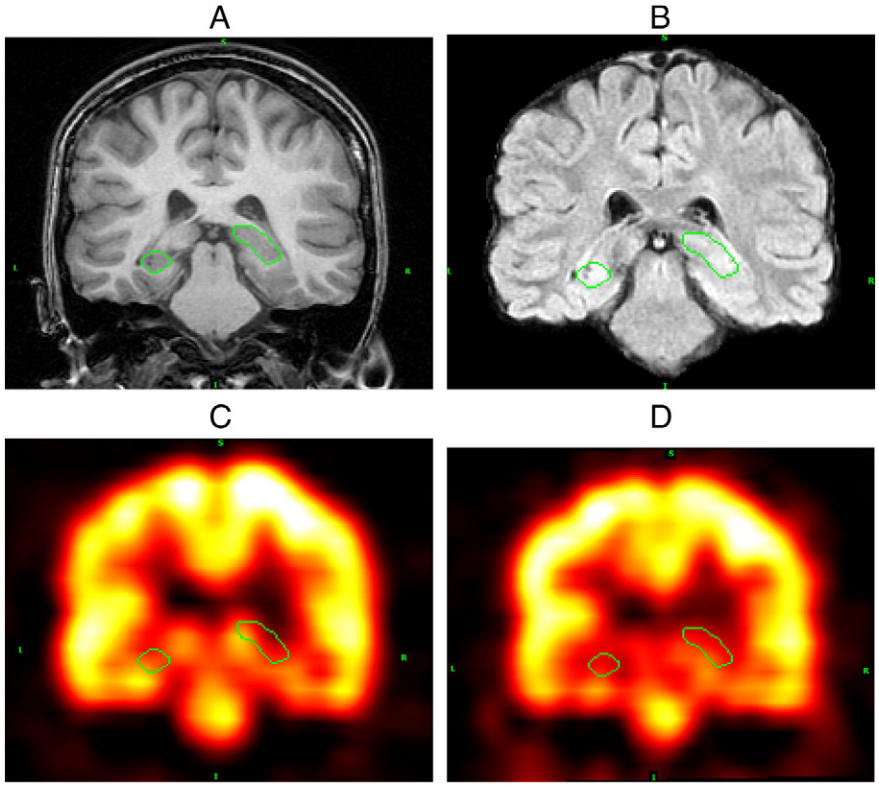

Fig. 1. Extraction of hippocampal volumes and FLAIR and SPECT intensities by co-registering the manually segmented hippocampi on T1-weighted image (A) to FLAIR (B), and ictal (C) and interictal (D) SPECT images using FLIRT [12].

data and the remaining 64 cases as training data [14]. The multinomial logistic models were regressed to training data as follows:

$$\ln\left(\frac{\Pr(Y_i = L|\, M_k)}{\Pr(Y_i = N|\, M_k)}\right) = \beta_L^k \cdot X_i, X_i^k \epsilon D \tag{1}$$

$$\ln\left(\frac{\Pr(Y_i = R|\, M_k)}{\Pr(Y_i = N|\, M_k)}\right) = \beta_R^k \cdot X_i, X_i^k \epsilon D \tag{2}$$

where X_i^k is a vector of i^{th} observation in training dataset D incorporated in Model k. $\Pr(Y_i = L|\, M_k)$, $\Pr(Y_i = R|\, M_k)$, and $\Pr(Y_i = N|\, M_k)$ are the posterior probabilities of the epileptogenic side Y_i being left (L), right (R), and neutral (N), respectively. β_L^k and β_R^k are the vectors of regression coefficients of Model k associated with X_i^k and the posterior probabilities. Since, in multinomial logistic regression, the epileptogenic side Y_i for each observation in training dataset was assumed to be known, the posterior probabilities $\Pr(Y_i = L|\, M_k)$, $\Pr(Y_i = R|\, M_k)$, and $\Pr(Y_i = N|\, M_k)$ were set to 0 or 1 depending on the decision made on the laterality. By estimation of coefficients β_L^k and β_R^k for Model k, the posterior probability of the epileptogenic side Y_j for jth validation data being left, right, or neutral were calculated, where

$$\Pr\left(Y_j = L|\, M_k\right) + \Pr\left(Y_j = R|\, M_k\right) + \Pr\left(Y_j = N|\, M_k\right) = 1. \tag{3}$$

The goodness-of-fit for the response models was assessed by the fit deviance as a generalized residual sum of squares.

2.5. Bayesian model averaging

Bayesian model averaging (BMA) constructs a model with a posterior probability by linearly weighting the posterior probabilities of multiple models [15]. Based on BMA, we developed imaging-based models as linear combinations of imaging-based response models:

$$\Pr\left(Y_j = S|\, D\right) = \sum_{k=1}^{T} \Pr\left(Y_j = S|\, M_k\right) \Pr(M_k|\, D) \tag{4}$$

where $S \epsilon \{L, R, N\}$ and T is the total number of models considered to make the posterior probability.

We used multinomial regression to estimate $\Pr(Y_j = S|\, M_k)$ using Eqs. (1) and (2). A difficulty associated with BMA involved estimating the posterior probability of model k given training dataset D, $\Pr(M_k|\, D)$. Using Bayes' theorem:

$$\begin{aligned}\Pr(M_k|\, D) &= \frac{\Pr(D|\, M_k)\Pr(M_k)}{\sum_{i=1}^{T}\Pr(D|\, M_i)\Pr(M_i)}\ ,\ \Pr(D|\, M_k)\\ &= \int \Pr(D|\, \theta_k, M_k)\Pr(\theta_k|\, M_k)d\theta_k\end{aligned} \tag{5}$$

where θ_k is the vector of regression parameters in Model k with $\Pr(\theta_k|\, M_k)$. The integrated likelihood $\Pr(D|\, M_k)$ can be estimated using the Bayesian information criterion (BIC) or Markov chain Monte Carlo (MCMC) method [15,16]. However, a distribution for the regression parameters θ_k (β_L^k and β_R^k in this application) has to be assumed properly. Instead of a model-based approach, we estimated the posterior probabilities for models $\Pr(M_k|\, D)$ in an observation-based approach.

$$\Pr\left(Y_j = S|\, D\right) = \sum_{k=1}^{T} \alpha_k \Pr\left(Y_j = S|\, M_k\right) \tag{6}$$

where α_k are the weighting coefficients subject to the constraint:

$$\sum_{k=1}^{T}\alpha_k = 1. \tag{7}$$

We considered the cost function £ to be minimized:

$$\begin{aligned}£ = &\sum_{j\epsilon L\_TLE}\left[1-\Pr\left(Y_j = L|\, D\right)\right]^2 + \left[\Pr\left(Y_j = R|\, D\right)\right]^2 + \left[\Pr\left(Y_j = N|\, D\right)\right]^2\\ &+\sum_{j\epsilon R\_TLE}\left[\Pr\left(Y_j = L|\, D\right)\right]^2 + \left[1-\Pr\left(Y_j = R|\, D\right)\right]^2 + \left[\Pr\left(Y_j = N|\, D\right)\right]^2\\ &+\sum_{j\epsilon Control}\left[\Pr\left(Y_j = L|\, D\right)\right]^2 + \left[\Pr\left(Y_j = R|\, D\right)\right]^2 + \left[1-\Pr\left(Y_j = N|\, D\right)\right]^2\end{aligned} \tag{8}$$

where L _ TLE, R _ TLE, and Control denote patients with left TLE, patients with right TLE, and control subjects, respectively. By inserting $\alpha_T = 1-\sum_{k=1}^{T-1}\alpha_k$ and Eq. (6) into Eq. (8), and taking the derivative with respect to α_i, T − 1 linear equations were generated from which the weighting coefficients α_k were estimated:

$$\begin{aligned}&\frac{\partial £}{\partial \alpha_i} = 0 \rightarrow \sum_{k=0}^{T-1} A_{ik}\alpha_k = 0 \qquad ,i = 1:T-1,\ \ \alpha_0 = 1\\ &A_{i0} = \sum_{j\epsilon L\_TLE}\Pr\left(Y_j = L|\, M_T\right) - \Pr\left(Y_j = L|\, M_i\right)\\ &\quad + \sum_{j\epsilon R\_TLE}\Pr\left(Y_j = R|\, M_T\right) - \Pr\left(Y_j = R|\, M_i\right)\\ &\quad + \sum_{j\epsilon Control}\Pr\left(Y_j = N|\, M_T\right) - \Pr\left(Y_j = N|\, M_i\right)\\ &\quad + \sum_{j\epsilon D}\Pr\left(Y_j = L|\, M_T\right)\left[\Pr\left(Y_j = L|\, M_i\right) - \Pr\left(Y_j = L|\, M_T\right)\right]\\ &\quad + \Pr\left(Y_j = R|\, M_T\right)\left[\Pr\left(Y_j = R|\, M_i\right) - \Pr\left(Y_j = R|\, M_T\right)\right]\\ &\quad + \Pr\left(Y_j = N|\, M_T\right)\left[\Pr\left(Y_j = N|\, M_i\right) - \Pr\left(Y_j = N|\, M_T\right)\right]\\ &A_{ik} = \sum_{j\epsilon D}\left[\Pr\left(Y_j = L|\, M_i\right) - \Pr\left(Y_j = L|\, M_T\right)\right]\\ &\quad \times\left[\Pr\left(Y_j = L|\, M_k\right) - \Pr\left(Y_j = L|\, M_T\right)\right]\\ &\quad + \left[\Pr\left(Y_j = R|\, M_i\right) - \Pr\left(Y_j = R|\, M_T\right)\right]\\ &\quad \times\left[\Pr\left(Y_j = R|\, M_k\right) - \Pr\left(Y_j = R|\, M_T\right)\right]\\ &\quad + \left[\Pr\left(Y_j = N|\, M_i\right) - \Pr\left(Y_j = N|\, M_T\right)\right]\\ &\quad \times\left[\Pr\left(Y_j = N|\, M_k\right) - \Pr\left(Y_j = N|\, M_T\right)\right]k = 1:T-1.\end{aligned} \tag{9}$$

We developed imaging-based Models 8 to 12 as various linear combinations of *independent* MRI- and SPECT-based response Models with optimal coefficients estimated based on observations.

- Model 8 attributes: posterior probabilities of 3 Models — 1, 2, and 3.
- Model 9 attributes: posterior probabilities of 3 Models — 1, 2, and 4.
- Model 10 attributes: posterior probabilities of 3 Models — 1, 3, and 4.
- Model 11 attributes: posterior probabilities of 3 Models — 2, 3, and 4.
- Model 12 attributes: posterior probabilities of 4 Models — 1, 2, 3, and 4.

For each validation dataset, by comparing the lateralization result Y_j with the correctly decided side, $Side_j$, we evaluated the performance of the response models by calculating the probability of detection and false alarm of the correct side for all subjects (Pr^D, Pr^{FA}), the probability of detection and false alarm of the epileptogenic side, the left and right epileptogenic sides for the TLE patients (Pr^D_{TLE}, Pr^{FA}_{TLE}, Pr^D_L, Pr^{FA}_L, Pr^D_R, Pr^{FA}_R, respectively), and the probability of detection and false alarm of the *Neutral* label for the control subjects (Pr^D_N, and Pr^{FA}_N) as:

$$\begin{aligned}Pr^D &= \frac{1}{n}\sum_{j=1}^{n}1\left(Y_j = L|\, Side_j = L\right) + 1\left(Y_j = R|\, Side_j = R\right)\\ &\quad +1\left(Y_j = N|\, Side_j = N\right)\\ Pr^{FA} &= \frac{1}{n}\sum_{j=1}^{n}1\left(Y_j = L|\, Side_j = R\right) + 1\left(Y_j = L|\, Side_j = N\right)\\ &\quad + 1\left(Y_j = R|\, Side_j = L\right) + 1\left(Y_j = R|\, Side_j = N\right)\\ &\quad + 1\left(Y_j = N|\, Side_j = L\right) + 1\left(Y_j = N|\, Side_j = R\right)\\ Pr^D_{TLE} &= \frac{1}{nL+nR}\sum_{j=1}^{n}1\left(Y_j = L|\, Side_j = L\right) + 1\left(Y_j = R|\, Side_j = R\right)\\ Pr^{FA}_{TLE} &= \frac{1}{nL+nR}\sum_{j=1}^{n}1\left(Y_j = L|\, Side_j = R\right) + 1\left(Y_j = R|\, Side_j = L\right)\\ Pr^D_L &= \frac{1}{nL}\sum_{j=1}^{n}1\left(Y_j = L|\, Side_j = L\right)\\ Pr^{FA}_L &= \frac{1}{nR+nC}\sum_{j=1}^{n}1\left(Y_j = L|\, Side_j = R\right) + 1\left(Y_j = L|\, Side_j = N\right)\\ Pr^D_R &= \frac{1}{nL}\sum_{j=1}^{n}1\left(Y_j = R|\, Side_j = R\right)\\ Pr^{FA}_R &= \frac{1}{nL+nC}\sum_{j=1}^{n}1\left(Y_j = R|\, Side_j = L\right) + 1\left(Y_j = R|\, Side_j = N\right)\\ Pr^D_N &= \frac{1}{nC}\sum_{j=1}^{n}1\left(Y_j = N|\, Side_j = N\right)\\ Pr^{FA}_N &= \frac{1}{nL+nR}\sum_{j=1}^{n}1\left(Y_j = N|\, Side_j = L\right) + 1\left(Y_j = N|\, Side_j = R\right).\end{aligned} \tag{10}$$

Table 1
Parameters of the response models.

Response models	Regression coefficients		Regression deviance
Model 1	$\beta^1_{0L} = 0.814$	$\beta^1_{0R} = -2.52$	68.1 ± 0.2
	$\beta^1_{1L} = -0.006$	$\beta^1_{1R} = 0.004$	
	$\beta^1_{2L} = 0.005$	$\beta^1_{2R} = -0.003$	
Model 2	$\beta^2_{0L} = 2.65$	$\beta^2_{0R} = -10.24$	65.5 ± 0.2
	$\beta^2_{1L} = 0.259$	$\beta^2_{1R} = -0.302$	
	$\beta^2_{2L} = -0.274$	$\beta^2_{2R} = 0.337$	
Model 3	$\beta^3_{0L} = -5.34$	$\beta^3_{0R} = -4.10$	104.8 ± 0.4
	$\beta^3_{1L} = 0.228$	$\beta^3_{1R} = 0.014$	
	$\beta^3_{2L} = -0.048$	$\beta^3_{2R} = 0.115$	
Model 4	$\beta^4_{0L} = -1.197$	$\beta^4_{0R} = -1.537$	65.1 ± 0.2
	$\beta^4_{1L} = 35.17$	$\beta^4_{1R} = -26.00$	
	$\beta^4_{2L} = -27.83$	$\beta^4_{2R} = 21.08$	
Model 5	$\beta^5_{0L} = 4.435$	$\beta^5_{0R} = -17.82$	32.9 ± 0.2
	$\beta^5_{1L} = 0.472$	$\beta^5_{1R} = -0.338$	
	$\beta^5_{2L} = -0.518$	$\beta^5_{2R} = 0.368$	
	$\beta^5_{3L} = 0.553$	$\beta^5_{3R} = -0.163$	
	$\beta^5_{4L} = -0.398$	$\beta^5_{4R} = 0.430$	
Model 6	$\beta^6_{0L} = 8.85$	$\beta^6_{0R} = -18.92$	25.9 ± 0.2
	$\beta^6_{1L} = -0.007$	$\beta^6_{1R} = 0.008$	
	$\beta^6_{2L} = 0.002$	$\beta^6_{2R} = -0.006$	
	$\beta^6_{3L} = 0.380$	$\beta^6_{3R} = -0.126$	
	$\beta^6_{4L} = -0.394$	$\beta^6_{4R} = 0.167$	
	$\beta^6_{5L} = 0.482$	$\beta^6_{5R} = -0.070$	
	$\beta^6_{6L} = -0.326$	$\beta^6_{6R} = 0.171$	
Model 7	$\beta^7_{0L} = -5.80$	$\beta^7_{0R} = -25.38$	11.9 ± 0.1
	$\beta^7_{1L} = -0.011$	$\beta^7_{1R} = 0.005$	
	$\beta^7_{2L} = 0.010$	$\beta^7_{2R} = -0.005$	
	$\beta^7_{3L} = 0.083$	$\beta^7_{3R} = -0.321$	
	$\beta^7_{4L} = -0.088$	$\beta^7_{4R} = 0.359$	
	$\beta^7_{5L} = 0.156$	$\beta^7_{5R} = -0.203$	
	$\beta^7_{6L} = 0.024$	$\beta^7_{6R} = 0.590$	
	$\beta^7_{7L} = 35.91$	$\beta^7_{7R} = -21.54$	
	$\beta^7_{8L} = -12.97$	$\beta^7_{8R} = 43.04$	

Table note: β^k_{jL} and β^k_{jR} are the regression coefficients j of Model k associated with X^k_i, the ith observation of the training dataset in Eqs. (1) and (2).

where *nL*, *nR*, *nC*, and *n* are the number of patients with left TLE, patients with right TLE, control subjects, and all subjects, respectively. 1(.) is a unit function with the value of 1 for true arguments and 0 otherwise.

3. Results

3.1. Single lateralization response Models

The regression coefficients of the response Models were estimated and listed in Table 1. Fig. 2 shows the regressed multinomial logistic function for the data points using univariate response Models 1 to 4 and multivariate response Model 7, along with the probability of the detected side being *Left*, *Right*, or *Neutral* for each TLE or control case. Table 2 shows the probability of detection and false alarm of lateralization for all subjects, the epileptogenic side, the left epileptogenic side, and the right epileptogenic side for TLE patients, and the Neutral label for control nonepileptic subjects. Among univariate response Models 1 to 4, response Model 4, with SPECT attributes, achieved the lowest fit deviance (65.1 ± 0.2; mean ± standard error), while response Models 1 and 2, with volumetrics and means of FLAIR intensity, reached the highest detection probability of 0.82 and lowest false alarm probability of 0.18 for the correct side in all subjects (Table 2).

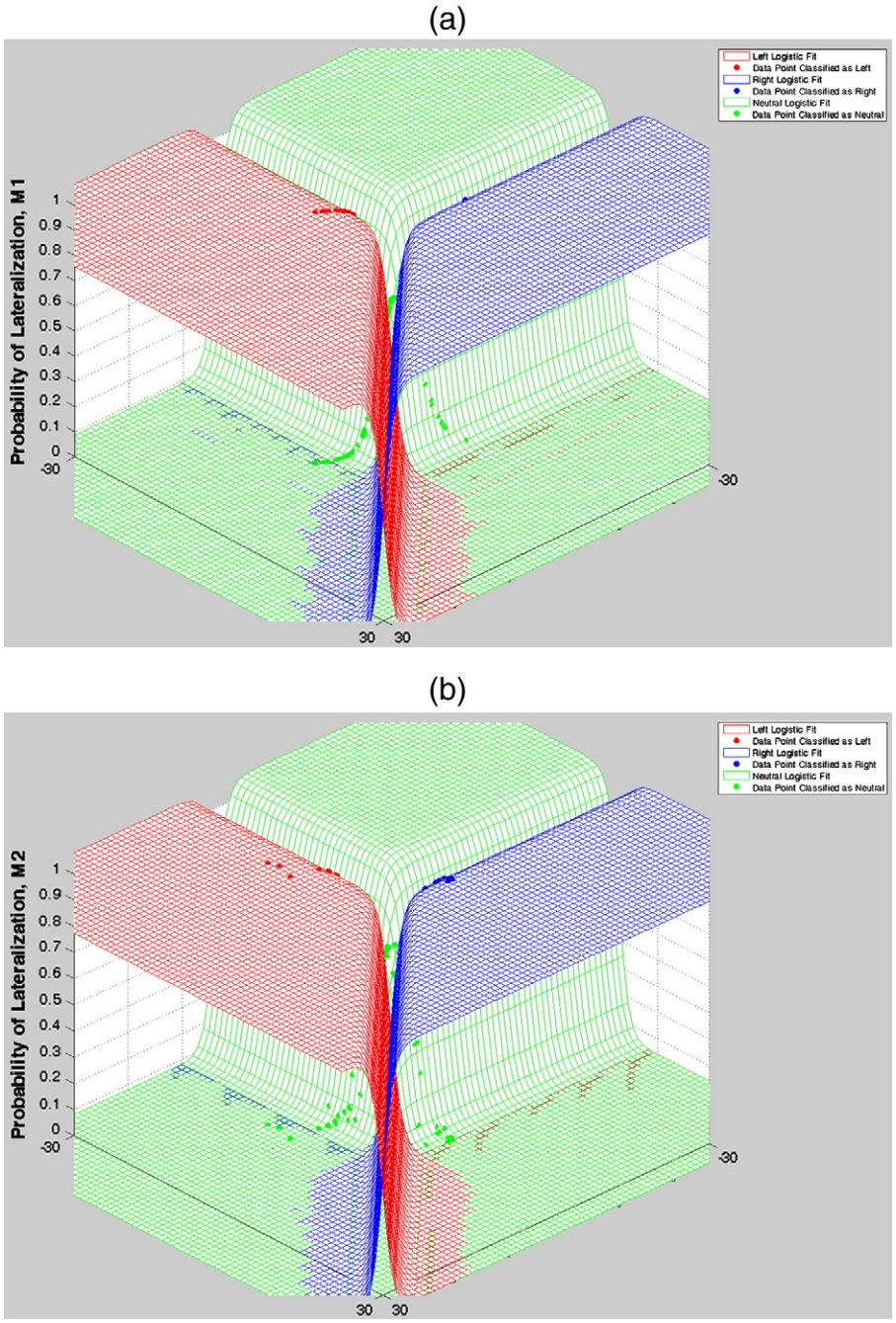

Fig. 2. Regressed multinomial logistic function to the data points using univariate response Models 1 (a), 2 (b), 3 (c), and 4 (d), and multivariate response Model 7 (e), along with the probability of detected side being *Left*, *Right*, or *Neutral* for each TLE or control case. The horizontal axes are the multivariate imaging feature space and the vertical axis is the probability of lateralization.

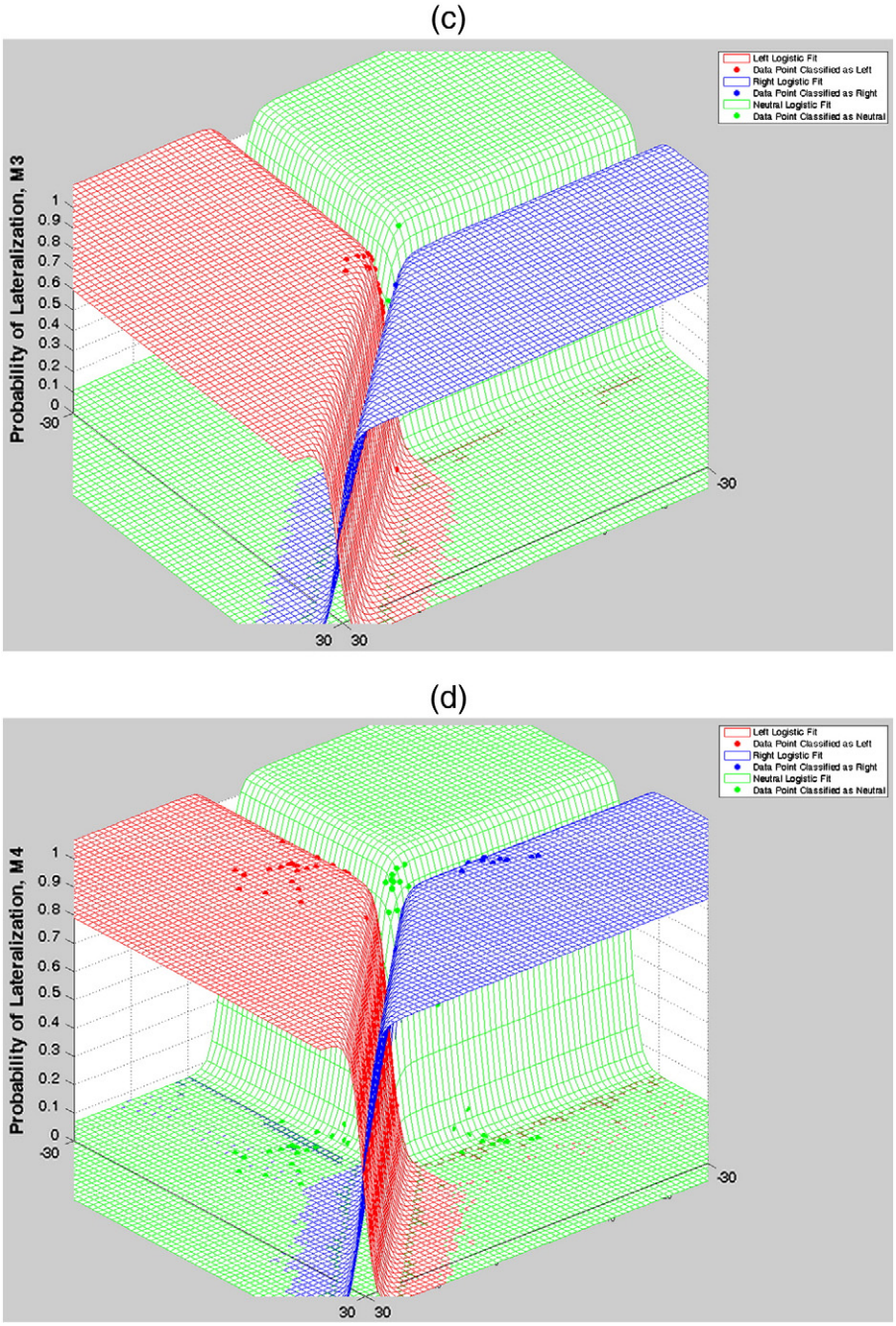

Fig. 2 (*continued*).

Integrating means and standard deviations of FLAIR, the bivariate response Model 5 outperformed both univariate response Models 2 and 3 (with means and standard deviations of FLAIR attributes, respectively) by achieving a higher probability of detection (0.94) as well as a lower probability of false alarm (0.06) for the correct side in all subjects (Table 2). The response Model 6 incorporating multivariate attributes of volumetrics, means and standard deviations of FLAIR intensity outperformed response Model 5 with means and standard deviations of FLAIR intensity by achieving a higher probability of detection (0.97) and a lower probability of false alarm (0.03) for the correct side in all subjects (Table 2). Incorporating all multivariate attributes of volumetrics, means and standard deviations of FLAIR intensity, and means of SPECT intensity, response Model 7 reached a significantly lower fit deviance (11.9 ± 0.1) than any other single response Model 1 to 6 ($p < 0.001$). It performed well in terms of achieving the probability of detection of 1 with no false alarms for the correct side in any subject and epileptogenicity in TLE patients (Table 2). As can be seen in Fig. 2, in this model more separability has been achieved for data points belonging to different classes of Left, Right, and Neutral in the multivariate imaging feature space, and the regressed multinomial logistic function did not misclassify any multivariate data point.

The averages of posterior probabilities for the *Left*, *Right*, and *Neutral* for the various response Models are presented in Table 3. The posterior probabilities of *Left, Right*, and *Neutral* along with the lower and upper limits of their confidence intervals have been depicted for univariate response Models 1 to 4, multivariate response Model 7, and BMA response

(e)

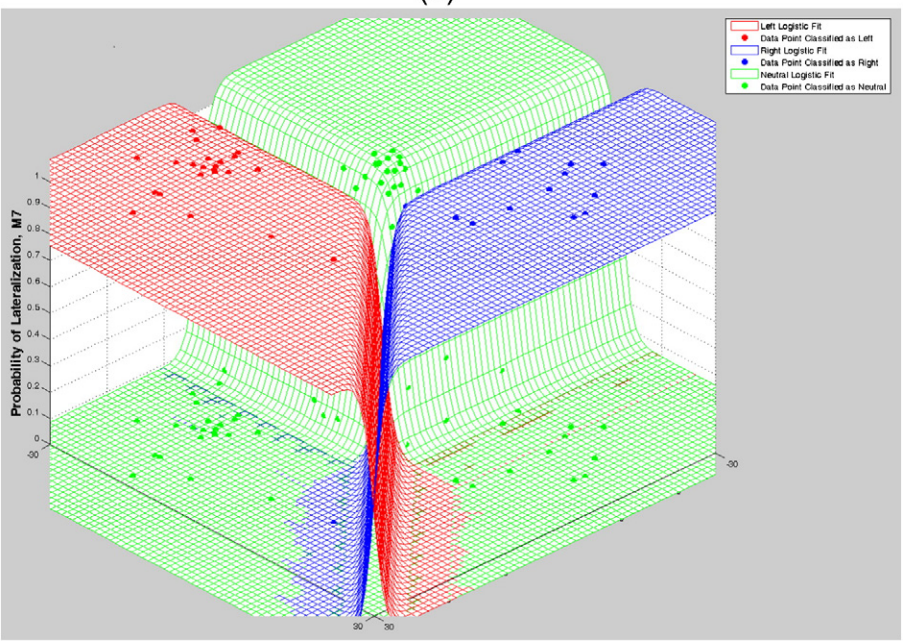

Fig. 2 (*continued*).

Model 12 in Fig. 3. As can be inferred from Table 3 and Fig. 3, response Model 7 assigned higher probabilities to the correct label, demonstrating high level of confidence in lateralization.

3.2. BMA lateralization response models

Table 4 shows the weighting coefficients estimated for BMA Models 8 to 12. Note that the coefficient corresponding to Model 3, with the standard deviation of FLAIR intensity, is negligible in the construction of BMA Models 8, 10, 11, and 12, demonstrating that Model 3 does not contribute adequately to the lateralization results of these models.

The BMA Model 9, composed of the three univariate Models 1, 2, and 4, and BMA Model 12, composed of the four univariate Models 1 to 4, reached the probability of detection of 1 with no false alarms (Table 3). In the construction of BMA Model 12, the univariate models, based on hippocampal volumes, means of hippocampal FLAIR intensity, and means of hippocampal SPECT intensity had comparable impacts (with estimated weighting coefficients 0.28, 0.32, and 0.31, respectively). However, the univariate model based on the standard deviation of hippocampal FLAIR had a negligible impact (with associated weighting coefficients 0.09) upon the process of lateralization. In the construction of BMA Model 9, the univariate models, based on hippocampal volumes, means of hippocampal FLAIR intensity, and means of hippocampal SPECT intensity had comparable impacts similar to BMA Model 12 (with corresponding weighting coefficients 0.29, 0.36, and 0.35, respectively) upon the process of lateralization.

Table 2
Lateralization results of various response models using leave-one-out cross-validation.

	M1	M2	M3	M4	M5	M6	M7	M8	M9	M10	M11	M12
Pr^{D}	0.82	0.82	0.71	0.80	0.94	0.97	1.00	0.89	1.00	0.94	0.94	1.00
Pr^{FA}	0.18	0.18	0.29	0.20	0.06	0.03	0.00	0.11	0.00	0.06	0.06	0.00
Pr^{D}_{TLE}	0.78	0.82	0.64	0.82	0.93	0.96	1.00	0.87	1.00	0.93	0.96	1.00
Pr^{FA}_{TLE}	0.02	0.02	0.18	0.02	0.00	0.02	0.00	0.02	0.00	0.02	0.02	0.00
Pr^{D}_{L}	0.86	0.82	0.79	0.89	0.96	0.96	1.00	0.86	1.00	1.00	0.96	1.00
Pr^{FA}_{L}	0.03	0.11	0.22	0.08	0.00	0.03	0.00	0.03	0.00	0.05	0.08	0.00
Pr^{D}_{R}	0.65	0.82	0.41	0.71	0.88	0.94	1.00	0.88	1.00	0.82	0.94	1.00
Pr^{FA}_{R}	0.04	0.02	0.06	0.06	0.02	0.00	0.00	0.02	0.00	0.00	0.00	0.00
Pr^{D}_{N}	0.90	0.80	0.85	0.75	0.95	1.00	1.00	0.95	1.00	0.95	0.90	1.00
Pr^{FA}_{N}	0.20	0.16	0.18	0.16	0.07	0.02	0.00	0.11	0.00	0.04	0.02	0.00

Table note: Pr^{D}, Pr^{FA}, Pr^{D}_{TLE}, Pr^{FA}_{TLE}, Pr^{D}_{L}, Pr^{FA}_{L}, Pr^{FA}_{R}, Pr^{D}_{R}, Pr^{D}_{N}, and Pr^{FA}_{N} represent the probability of detection and false alarm of the lateralization for all subjects, the epileptogenic side, the left epileptogenic side, and the right epileptogenic side for TLE patients, and the neutral label for control nonepileptic subjects, respectively. M1 to M12 denote response Models 1 to 12, resectively.

3.3. Clinical decision-making on laterality based on response Models

Response Models 7, 9, or 12, detected the epileptogenic side for all 15 patients who had undergone phase II evaluation (i.e., intracranial monitoring). Sixty percent in this group showed no discrepancy in lateralization results using response Models 1 to 7. Moreover, the side of epileptogenicity was detected for all 30 patients who had undergone only phase I of EEG monitoring with no false alarms raised for detection of left or right sides. Ninety-three percent of this latter group were also in agreement with the results of other response models.

4. Discussion and conclusion

In this work, univariate and multivariate response-driven lateralization models were proposed based on hippocampal MRI and SPECT attributes. Multinomial logistic regression and Bayesian model averaging were used to determine the side of epileptogenicity in temporal lobe epilepsy patients. We showed, by lateralization of the epileptogenic side using the proposed response models that this process succeeded in establishing laterality in all cases that had required intracranial monitoring to define the site of epileptogenicity, raising the notion that the latter might be supplanted, at least in some cases, by such an approach. Prior study has suggested the same while indicating the ultimate need for intracranial monitoring in cases of nonlesional extratemporal cases, in particular [17]. The proposed response model also proved reliable for those patients who had undergone only phase I EEG monitoring, affirming the side of epileptogenicity for all with no false alarms.

Table 3
Mean ± standard error of posterior probalilities of *Left*, *right*, and *Neutral* for various response models.

	M1	M2	M3	M4	M5	M6	M7	M8	M9	M10	M11	M12
$Pr(\mathbf{Y} = \mathbf{L} \mid \mathbf{Side} = \mathbf{L}, \mathbf{M_k})$	0.84 ± 0.05	0.77 ± 0.05	0.64 ± 0.06	0.82 ± 0.05	0.92 ± 0.04	0.94 ± 0.03	0.98 ± 0.01	0.80 ± 0.04	0.80 ± 0.03	0.82 ± 0.03	0.78 ± 0.04	0.79 ± 0.03
$Pr(\mathbf{Y} = \mathbf{R} \mid \mathbf{Side} = \mathbf{L}, \mathbf{M_k})$	0.04 ± 0.02	0.04 ± 0.02	0.16 ± 0.04	0.03 ± 0.02	0.00 ± 0.00	0.01 ± 0.00	0.00 ± 0.00	0.04 ± 0.01	0.03 ± 0.01	0.04 ± 0.01	0.04 ± 0.01	0.05 ± 0.01
$Pr(\mathbf{Y} = \mathbf{N} \mid \mathbf{Side} = \mathbf{L}, \mathbf{M_k})$	0.12 ± 0.04	0.20 ± 0.04	0.20 ± 0.04	0.15 ± 0.04	0.08 ± 0.04	0.05 ± 0.03	0.02 ± 0.01	0.16 ± 0.03	0.16 ± 0.02	0.14 ± 0.02	0.18 ± 0.03	0.16 ± 0.02
$Pr(\mathbf{Y} = \mathbf{L} \mid \mathbf{Side} = \mathbf{R}, \mathbf{M_k})$	0.10 ± 0.05	0.06 ± 0.05	0.29 ± 0.06	0.05 ± 0.03	0.06 ± 0.05	0.03 ± 0.02	0.00 ± 0.00	0.08 ± 0.04	0.07 ± 0.02	0.09 ± 0.03	0.07 ± 0.03	0.09 ± 0.02
$Pr(\mathbf{Y} = \mathbf{R} \mid \mathbf{Side} = \mathbf{R}, \mathbf{M_k})$	0.61 ± 0.08	0.77 ± 0.08	0.42 ± 0.04	0.68 ± 0.08	0.86 ± 0.07	0.87 ± 0.07	0.96 ± 0.02	0.69 ± 0.05	0.69 ± 0.04	0.63 ± 0.05	0.72 ± 0.04	0.66 ± 0.04
$Pr(\mathbf{Y} = \mathbf{N} \mid \mathbf{Side} = \mathbf{R}, \mathbf{M_k})$	0.30 ± 0.05	0.16 ± 0.05	0.29 ± 0.04	0.27 ± 0.06	0.08 ± 0.04	0.10 ± 0.05	0.04 ± 0.02	0.23 ± 0.03	0.24 ± 0.02	0.29 ± 0.03	0.22 ± 0.03	0.25 ± 0.02
$Pr(\mathbf{Y} = \mathbf{L} \mid \mathbf{Side} = \mathbf{N}, \mathbf{M_k})$	0.14 ± 0.03	0.27 ± 0.04	0.25 ± 0.02	0.21 ± 0.05	0.06 ± 0.02	0.06 ± 0.02	0.02 ± 0.01	0.21 ± 0.03	0.22 ± 0.02	0.18 ± 0.02	0.25 ± 0.03	0.22 ± 0.02
$Pr(\mathbf{Y} = \mathbf{R} \mid \mathbf{Side} = \mathbf{N}, \mathbf{M_k})$	0.28 ± 0.03	0.14 ± 0.03	0.28 ± 0.01	0.23 ± 0.04	0.11 ± 0.03	0.10 ± 0.03	0.04 ± 0.01	0.21 ± 0.03	0.21 ± 0.02	0.26 ± 0.02	0.19 ± 0.02	0.22 ± 0.02
$Pr(\mathbf{Y} = \mathbf{N} \mid \mathbf{Side} = \mathbf{N}, \mathbf{M_k})$	0.57 ± 0.01	0.58 ± 0.02	0.47 ± 0.02	0.55 ± 0.03	0.82 ± 0.03	0.84 ± 0.03	0.94 ± 0.01	0.58 ± 0.01	0.57 ± 0.02	0.56 ± 0.02	0.57 ± 0.02	0.56 ± 0.02

Table note: M1 to M12 denote response Models 1 to 12, resectively.

Bayesian model averaging (BMA) accounts for the uncertainty associated with single models by weighing their posterior model probabilities [15]. It has been shown that BMA outperforms single models on new observations in theory [18] and practice [15]. In our acquired dataset, a less complicated single multivariate model, incorporating all multivariate attributes, performed as well as the BMA model, incorporating all univariate models of those attributes, in achieving the probability of detection of 'one' with no false alarms for establishing the laterality of epileptogenicity in TLE patients. Nevertheless, our aim was to introduce a potential framework with the application of BMA in lateralization of the epileptogenic side in TLE patients that can quantify how much different imaging modalities are weighted in decision-making to achieve a better outcome.

Successful surgical treatment of focal epilepsy requires a reliable localization of seizure onset which, in the case of TLE, often amounts to a proper lateralization of the causative pathophysiology. The process of epileptogenesis and the subsequent epileptogenicity expressed in the mesial temporal structure brings about alterations in tissue properties, some of which may be characterized by imaging attributes rendered by various MR and SPECT postprocessing applications. Each technique by itself, however, provides only a limited perspective upon the condition and each has inherent weaknesses in its respective application [11]. Ostensibly, a multimodal imaging approach would enhance lateralization capability by accruing data, which, if concordant, would provide the required confirmation to proceed with either intracranial electrographic study targeting the appropriate area or to proceed directly with resective surgery in those cases where electrophysiological attributes were in agreement. As such, a multimodal integrative approach could reduce the magnitude of the required surgical exposure and, in some cases, even forego the need for invasive monitoring [19].

A number of studies have addressed the comparative and combined strengths of various individual imaging studies in cases where nonlesional EEG and MRI findings were present. Proton magnetic resonance spectroscopy (^{1}HMRS) has been shown concordant with EEG in MRI-negative unilateral TLE in 60–75% of cases [17,20,21]. Group comparisons of the diagnostic accuracy of temporal metabolite changes studied by Linear Combination of Model Spectra via water reference in TLE and control cases show reduced N-acetylaspartate (NAA) and elevated choline in the epileptogenic temporal lobe [21]. Despite this, ^{1}HMRS itself has not correlated well with seizure outcome, demonstrating a poor predictive value [17]. Hippocampal atrophy, on the other hand, has been shown to strongly correlate with seizure-free outcome and, when combined with ^{1}HMRS, has demonstrated lateralization in 83% of cases [22]. Positron emission tomography (PET) lateralized 87% of TLE cases in a prospective study of 23 patients with age-matched controls, better than what was possible using hippocampal volumetry (65%); however, only 6/10 cases with nonlateralizing MRI study could be correlated with scalp EEG [22]. Although both PET and ^{1}HMRS were capable of lateralizing the site of epileptogenicity in TLE patients with nonlateralizing MRI study, only hippocampal volumetry was found predictive of a seizure-free outcome. Lateralization by single photon emission computed tomography (SPECT) has been found concordant with EEG in 84% of MRI-positive and 67% of MRI-negative TLE patients [20]. The concordance rate of ^{1}HMRS and SPECT in unilateral TLE patients was 74% in MRI-positive and 67% in MRI-negative situations. Contralateral findings with each modality, however, were identified in almost 30% of patients. Concordance of these imaging modalities with EEG was found highly predictive of a favorable postoperative outcome. Hippocampal fluid-attenuated inversion recovery (FLAIR) MRI lateralization accuracy when using both mean signal intensity and standard deviation has been shown to be 75% when control cases were used to establish a boundary domain within which study cases were deemed inconclusive [4]. Using a similar approach with subtraction SPECT coregistered to MRI, a lateralization accuracy of 89% was achieved for patients attaining a seizure-free outcome [5]. Interestingly, no significant correlation arose between hippocampal FLAIR MRI and

SPECT suggesting that the two modalities bore complementary information. More recently, reduced fractional anisotropy detected in the inferolateral cingulum ipsilateral to mesial temporal epileptogenicity, has been shown to be a strong indicator of laterality in mTLE, including cases without hippocampal sclerosis [23]. Unique in this approach was an assessment of interhemispheric variation uncertainty (HVU) to ensure that a true quantitative difference existed for the individual patient. Such assurances may prove worthwhile in all quantitative applications involving comparisons of bilateral structures.

In cases where imaging modalities are discordant regarding laterality or by the absence of any distinguishing attribute, the clinician must weigh the relative contributions of each modality and assign a qualitative estimate upon the reliability of each in relation to electrophysiological findings. Most studies to-date have used simple asymmetry analysis of an imaging index in a bilateral structure such as the hippocampus and showed its concordance with scalp or intracranial EEG as a gold standard but did not integrate multimodal findings into a comprehensive multivariate lateralization framework [17,20–22]. Agreement regarding lateralization among imaging studies enhances confidence in decision-making and is predictive of a favorable outcome [24], whereas, discordance creates uncertainty in decision-making in the absence of a definable scheme by which to judge the relative contributions of each. Other multimodal studies adopted a hierarchical scoring scheme for individual modalities. Positive evidence of laterality with each modality was regarded equally and a notation of inter-modality concordance was derived [9,10,19,24]. Semiquantitative scores and a quantitative Bayesian framework using conditional probabilities and likelihood ratios constitute a more refined approach. Using such Bayesian probabilistic reasoning, one can estimate the diagnostic worth of individual lateralization methods in numerical terms for the purpose of cross-modality comparisons [9,10]. The quantitative approach in all of these multimodal applications assigns a score of zero or one to the lateralization results of individual modalities as a measure of a distinguishing attribute. A weighted integration scheme that assigns a probability for each individual modality, however, would provide a more realistic model by which to judge the outcome of the investigation.

Multimodal postprocessing can incorporate the information of multiple modalities simultaneously without having to assign a posterior probability to the lateralization result of any individual modality. It overcomes the intrinsic limitation of individual modalities such as the

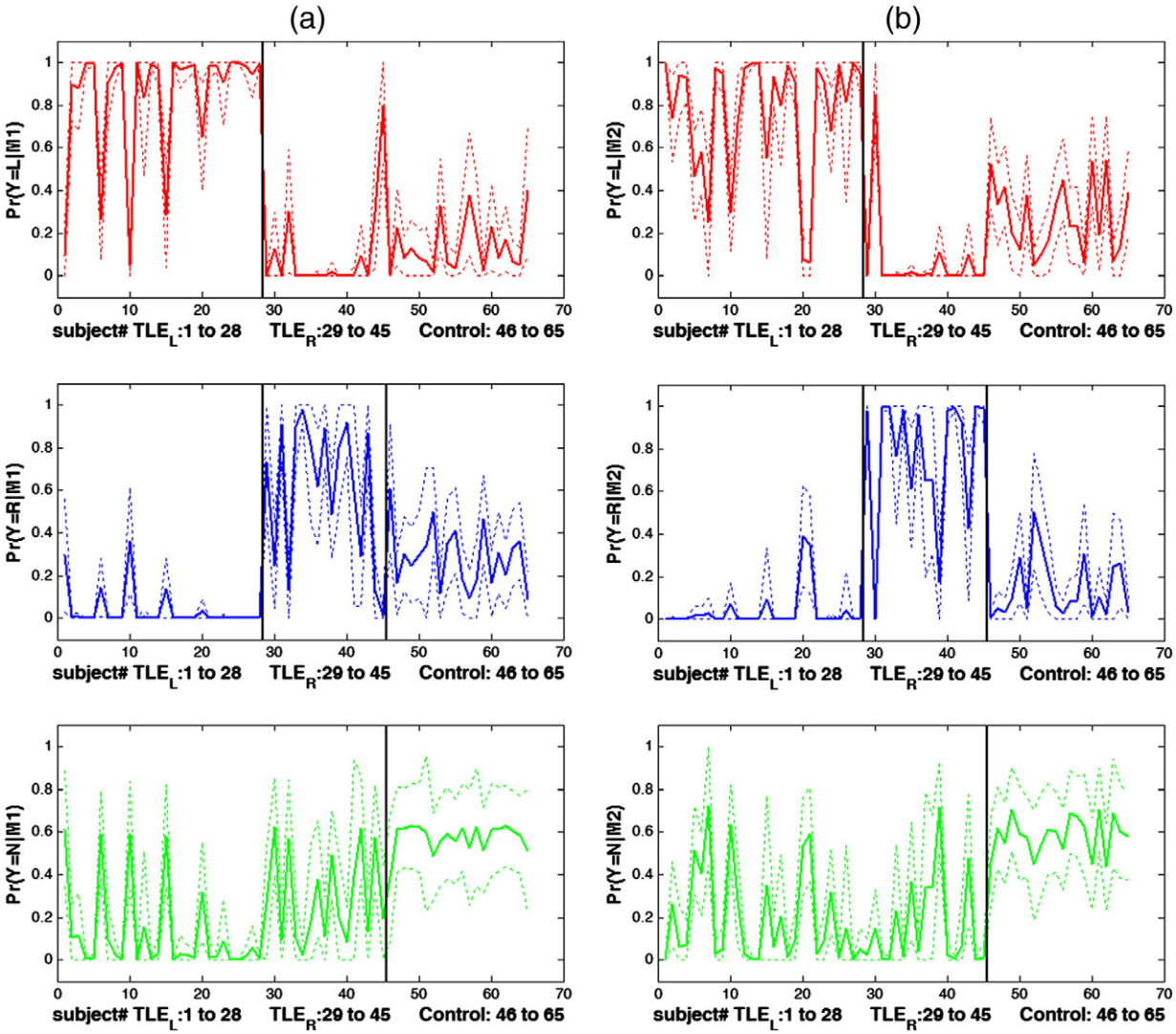

Fig. 3. Posterior probabilities (solid lines) of *Left* (red), *Right* (blue), and *Neutral* (green) along with the lower and upper limits of their confidence interval (dash lines) for univariate response Models 1 (a), 2 (b), 3 (c), 4 (d), multivariate response Model 7 (e), and BMA response Model 12 (f).

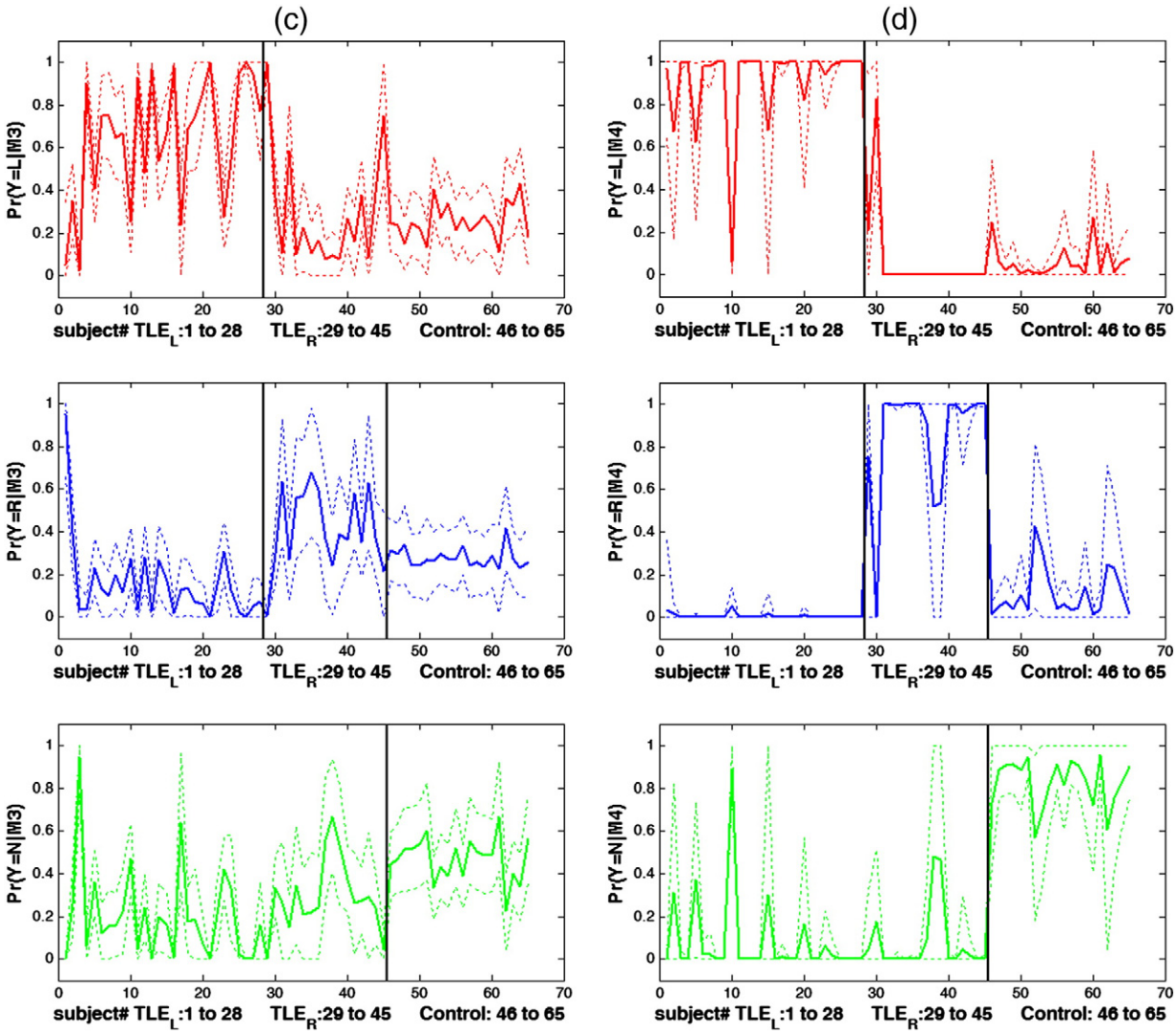

Fig. 3 (*continued*).

inherent sensitivity, specificity, temporal resolution, and spatial resolution to increase the information content made available in order to draw a conclusion [11]. Scalp EEG is a vital component of the investigation of focal epilepsy, offering excellent temporal resolution in milliseconds, but apart from the limitations in its recording and interpretation, the poor spatial resolution detracts from its sole use as a localizing modality [11].

The presence of variability in quantitative hippocampal imaging indices can be attributed to imaging system-specific or subject-specific factors. Supposing the left and right hippocampi undergo the same imaging conditions, the hippocampal interhemispheric variations in imaging indices in epilepsy patients can be related to subject-specific factors including natural physiological occurrences and to actual epileptogenicity expressed variably in each hippocampus. In order to establish that lateralization response models actually lateralize the site of epileptogenicity based upon pathology-induced interhemispheric variation in the case of a unilateral TLE, we incorporated into the proposed lateralization response models the imaging indices of a cohort of control, nonepileptic subjects who had undergone their studies with the same scanner and imaging parameters. Variability for any natural physiological occurrences would therefore be taken into account in the modeling. Under these circumstances, the proposed multinomial response models can more confidently reflect the predominance of pathological effects in lateralizing the epileptogenic site. On the other hand, in the case of a neutral label, a physiological effect is most probably predominant even in the presence of interhemispheric variation among any of the imaging modalities.

Funding statement

This work was supported in part by NIH grant R01-EB013227.

Ethics approval

Ethics approval was provided by Henry Ford Health System Institutional Review Board, Detroit, Michigan, USA.

Conflict of interest

There is no conflict of interest to report.

Acknowledgments

Special thanks to Kourosh Jafari-Khouzani, Mohammad-Parsa Hosseini, Hajar Hamidian, Abdelrahman Hassane, Oltion Meci, and Harrini Vijay for their invaluable help in data processing.

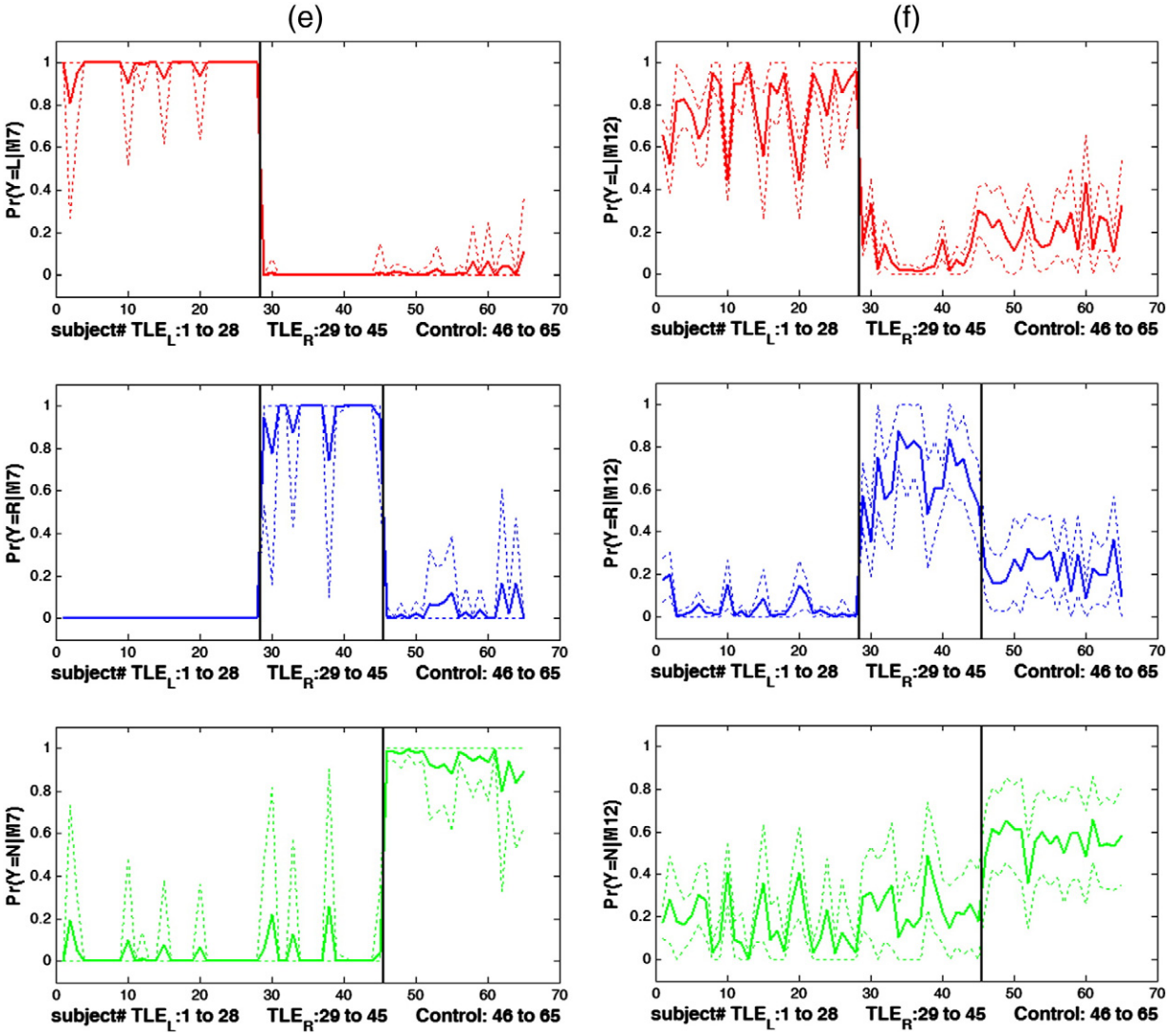

Fig. 3 (*continued*).

Table 4
Weighting coefficients assigned to various BMA Models 8 to 12.

	Model 8	Model 9	Model 10	Model 11	Model 12
Constructing models and coefficients	α_1Model$_1$ $+\alpha_2$Model$_2$ $+\alpha_3$Model$_3$	α_1Model$_1$ $+\alpha_2$Model$_2$ $+\alpha_3$Model$_4$	α_1Model$_1$ $+\alpha_2$Model$_3$ $+\alpha_3$Model$_4$	α_1Model$_2$ $+\alpha_2$Model$_3$ $+\alpha_3$Model$_4$	α_1Model$_1$ $+\alpha_2$Model$_2$ $+\alpha_3$Model$_3$ $+\alpha_3$Model$_4$
α_1	0.46	0.29	0.48	0.51	0.28
α_2	0.53	0.36	0.07	0.04	0.32
α_3	0.01	0.35	0.45	0.45	0. 09
α_4	–	–	–	–	0.31

References

[1] Engel Jr J. Surgery for seizures. N Engl J Med 1996;334(10):647–53.
[2] Akhondi-Asl A, Jafari-Khouzani K, Elisevich K, Soltanian-Zadeh H. Hippocampal volumetry for lateralization of temporal lobe epilepsy: automated versus manual methods. Neuroimage 2011;54:S218–26.
[3] Lopez-Acevedo ML, Martinez-Lopez M, Favila R, Roldan-Valadez E. Secondary MRI-findings, volumetric and spectroscopic measurements in mesial temporal sclerosis. Swiss Med Wkly 2012;142:w13549.
[4] Jafari-Khouzani K, Elisevich K, Patel S, Smith B, Soltanian-Zadeh H. FLAIR signal and texture analysis for lateralizing mesial temporal lobe epilepsy. Neuroimage 2010; 49(2):1559–71.
[5] Jafari-Khouzani K, Elisevich K, Karvelis KC, Soltanian-Zadeh H. Quantitative multi-compartmental SPECT image analysis for lateralization of temporal lobe epilepsy. Epilepsy Res 2011;95(1):35–50.
[6] Bulacio JC, Jehi L, Wong C, Gonzalez-Martinez J, Kotagal P, Nair D, et al. Long-term seizure outcome after resective surgery in patients evaluated with intracranial electrodes. Epilepsia 2012;53(10):1722–30.
[7] Arya R, Mangano FT, Horn PS, Holland KD, Rose DF, Glauser TA. Adverse events related to extraoperative invasive EEG monitoring with subdural grid electrodes: a systematic review and meta-analysis. Epilepsia 2013;54(5):828–39.
[8] Kuzniecky R, Bilir E, Gilliam F, Faught E, Palmer C, Morawetz R, et al. Multimodality MRI in mesial temporal sclerosis: relative sensitivity and specificity. Neurology 1997;49(3):774–8.
[9] Kalamangalam GP, Knight EMP, Visweswaran S, Gupta A. Noninvasive predictors of subdural grid seizure localization in children with nonlesional focal epilepsy. J Clin Neurophysiol 2013;30(1):45–50.
[10] Kalamangalam GP, Morris III HH, Mani J, Lachhwani DK, Visweswaran S, Bingaman WM. Noninvasive correlates of subdural grid electrographic outcome. J Clin Neurophysiol 2009;26(5):333–41.
[11] Olson LD, Perry MS. Localization of epileptic foci using multimodality neuroimaging. Int J Neural Syst 2013;23(01).
[12] Jenkinson M, Smith S. A global optimisation method for robust affine registration of brain images. Med Image Anal 2001;5(2):143–56.
[13] Hosmer Jr DW, Lemeshow S, Sturdivant RX. Applied logistic regression. www.wiley.com; 2013.
[14] Picard RR, Cook RD. Cross-validation of regression models. J Am Stat Assoc 1984; 79(387):575–83.
[15] Raftery AE. Bayesian model selection in social research. Sociol Methodol 1995;25: 111–64.

[16] Yeung KY, Bumgarner RE, Raftery AE. Bayesian model averaging: development of an improved multi-class, gene selection and classification tool for microarray data. Bioinformatics 2005;21(10):2394–402.
[17] Zhang J, Liu Q, Mei S, Zhang X, Liu W, Chen H, et al. Identifying the affected hemisphere with a multimodal approach in MRI-positive or negative, unilateral or bilateral temporal lobe epilepsy. Neuropsychiatr Dis Treat 2014;10:71.
[18] Madigan D, Raftery AE. Model selection and accounting for model uncertainty in graphical models using Occam's window. J Am Stat Assoc 1994;89(428):1535–46.
[19] Jayakar P, Dunoyer C, Dean P, Ragheb J, Resnick T, Morrison G, et al. Epilepsy surgery in patients with normal or nonfocal MRI scans: integrative strategies offer long-term seizure relief. Epilepsia 2008;49(5):758–64.
[20] Doelken M, Richter G, Stefan H, Doerfler A, Noemayr A, Kuwert T, et al. Multimodal coregistration in patients with temporal lobe epilepsy—results of different imaging modalities in lateralization of the affected hemisphere in MR imaging positive and negative subgroups. Am J Neuroradiol 2007;28(3):449–54.
[21] Hammen T, Kerling F, Schwarz M, Stadlbauer A, Ganslandt O, Keck B, et al. Identifying the affected hemisphere by 1H-MR spectroscopy in patients with temporal lobe epilepsy and no pathological findings in high resolution MRI. Eur J Neurol 2006;13(5):482–90.
[22] Knowlton RC, Laxer KD, Ende G, Hawkins RA, Wong ST, Matson GB, et al. Presurgical multimodality neuroimaging in electroencephalographic lateralized temporal lobe epilepsy. Ann Neurol 1997;42(6):829–37.
[23] Nazem-Zadeh MR, Schwalb JM, Elisevich KV, Bagher-Ebadian H, Hamidian H, Akhondi-Asl AR, et al. Lateralization of temporal lobe epilepsy using a novel uncertainty analysis of MR diffusion in hippocampus, cingulum, and fornix, and hippocampal volume and FLAIR intensity. J Neurol Sci 2014;342(1-2):152–61.
[24] Diehl B, Lüders H. Temporal lobe epilepsy: when are invasive recordings needed? Epilepsia 2000;41(s3):S61–74.